Proposal for Graphene–Boron Nitride Heterobilayer-Based Tunnel FET

Ram Krishna Ghosh and Santanu Mahapatra, *Senior Member, IEEE*

***Abstract*—We investigate the gate-controlled direct band-to-band tunneling (BTBT) current in a graphene–boron nitride (G-BN) heterobilayer channel-based tunnel field effect transistor. We first study the imaginary band structure of hexagonal and Bernal-stacked heterobilayers by density functional theory, which is then used to evaluate the gate-controlled current under the Wentzel–Kramers–Brillouin approximation. It is shown that the direct BTBT is probable for a certain interlayer spacing of the G-BN which depends on the stacking orders.**

***Index Terms*—Band-to-band tunneling, complex band structure, graphene, tunnel field effect transistor (TFET).**

I. Introduction

TUNNEL field effect transistors (TFETs) have appeared as a strong candidate for the next-generation low stand by power (LSTP) applications due to their sub-60-mV/dec sub-threshold slope (SS) [1], [2]. However, the large indirect energy band gap of silicon makes it difficult to achieve low SS and high-ON current from the conventional silicon TFETs. As a result, alternative channel materials for the TFET are being investigated, which might have lower value of "least action integral" [3] and do not require phonon assistance for carrier tunneling. In the recent past, carbon-based materials especially carbon nanotube and graphene nanoribbon (GNR) find much attraction in the TFET applications [1], [4]– [6]. Though the ultrahigh carrier mobility of the graphene has attracted extensive interest, its zero band gap E_g feature has made it difficult for the transistor applications. Thus, opening and tailoring a band gap has become a highly pursued topic in the recent graphene research. A vertical external electric field can induce a tunable E_g of up to 0.25eV for the bilayer graphene (GBL) [7], however, it also increases the carrier effective mass. Based on the GBL, recently, Fiori and Iannaccone [8] have proposed an ultra-low-voltage TFET. Earlier, it was investigated that, instead of GBL, a graphene-boron nitride heterobilayer (HBL) can produce quite higher E_g and carrier mobility depending on their interlayer spacing and stacking pattern [9]–[11].

In this letter, we explore the BTBT in an HBL by considering the complex dispersion relationship within the band gap region, which is evaluated by Atomistix ToolKit using the density functional theory (DFT) [12]. Finding the least action integral from the atomistic simulation and considering the analytical Poisson solution, we compute the drain current of a symmetric double gate (DG) TFET [see Fig. 1(a)] and compare the performances for different interlayer spacing and their stacking pattern.

Manuscript received March 4, 2013; accepted July 3, 2013. Date of publication July 11, 2013; date of current version September 4, 2013. This work was supported by the Department of Science and Technology, Government of India, under Grant SR/S3/EECE/0151/2012. The review of this paper was arranged by Associate Editor Dr. A. Martinez.

The authors are with the Nano-Scale Device Research Laboratory, Department of Electronic Systems Engineering, Indian Institute of Science, Bangalore-560012, India (e-mail: ramki.phys@gmail.com; santanu@cedt.iisc.ernet.in).

Color versions of one or more of the figures in this paper are available online at http://ieeexplore.ieee.org.

Digital Object Identifier 10.1109/TNANO.2013.2272739

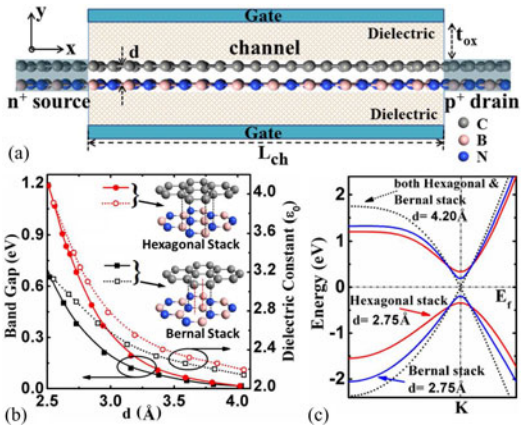

Fig. 1. (a) Schematic cross section of an HBL-based DG TFET with n^+ source, p^+ drain, and intrinsic channel. (b) Plot of the energy band gaps and static dielectric constants as function of d. (c) Electronic band structure of an HBL for different d and stacking pattern.

II. Methodology, Results, and Discussions

The electronic band structure of the geometrically optimized HBL graphene is calculated by the DFT method combining with local density approximation and double zeta polarized basis set. The k-point sampling of a $21 \times 21 \times 1$ grid is used with a mesh cutoff energy of 10 Hartree. In addition, the tolerance parameter 10^{-5} with maximum steps of 200 is used as the iteration control parameter. Like the GBL, in our study, we consider two types of stacking patterns [Hexagonal (AA) and Bernal stacking (AB)] as shown in Fig. 1. Though there are possibilities for some more stacking patterns, using the DFT it is demonstrated that AB-stacked HBL is more stable one [9], [11]. Thus, in this letter, we consider only two stacking patterns: AB, which is most stable and AA that has the minimum state with slightly higher energy. It has been observed that both interlayer spacing d as well as stacking pattern play crucial roles in the band gap opening. It can be seen from Fig. 1(b) that when d is large enough ($\sim 4.2\AA$), there are not much interlayer interactions between the graphene and boron nitride layers and the band lines are almost identical to those of the graphene monolayer. With the decrease of d, the interlayer interactions become stronger and it opens a band gap and shows a quasi-parabolic dispersion near the Fermi level [see Fig. 1(c)]. Therefore, the electronic band structure of an HBL is mainly dictated by the graphene layer. Fig. 1(b) shows that the band gaps increase with the decrease in d but the increment in AA is much higher than the AB due to the presence of stronger orbital interactions in AA than AB [11]. We have also investigated the static dielectric constant (ε) of an HBL from the optical spectrum (using DFT-LDA) and observed similar trend as shown in Fig. 1(b).

Recently, the complex band theory within the band gap has been used for better understanding of the BTBT phenomenon and modeling tunneling devices. Physically, during this BTBT process, when a carrier tunnels through a band gap region, it

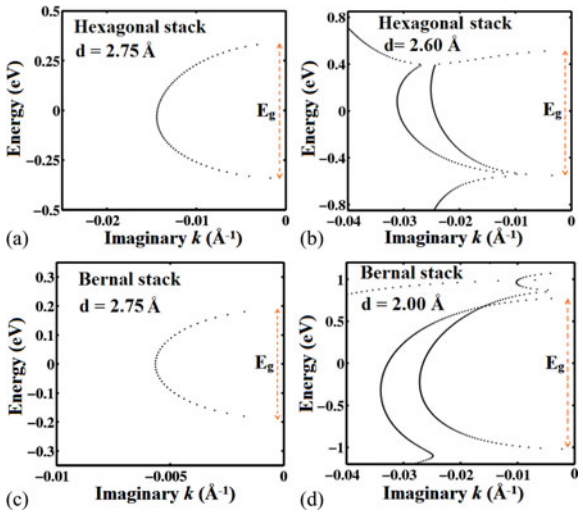

Fig. 2. Complex bands within the forbidden gap (E_g) of an HBL having (a)–(b) AA and (c)–(d) AB stacking.

transits in an evanescent mode and its wave vector becomes imaginary within this forbidden gap. It should be noted that the interband tunneling probability (T_{BTBT}) depends on the minimum area that is enclosed by the complex band which connects the valence band edge to the conduction band edge [13], [14]. Fig. 2 shows the complex band within the band gap region of an HBL for both AA- and AB-stacking patterns. For the clarity of the band structures, only few bands are represented here. It is worth noting that in the case of direct band gap semiconductors when the complex band that starts from the top of valence band "*wraps*" itself to the bottom of the conduction band, constituting one continuous band, then only the direct band-to-band tunneling can be possible, whereas, when the band that starts from the valence band edge does not end up at the conduction band edge, rather "*crosses*" with the band starting from the conduction band edge, then the inclusion of phonon exchange is required in the tunneling process which reduces the transmission rate quite significantly [13], [14]. Now, it appears from Fig. 2(a) and (c) that, in the case of both the AA- and AB-stacked HBL, the complex band is characterized by a continuous band that connects the highest valence subband to the lowest conduction subband and makes the tunneling as a direct one. However, with the decrease of d, the tunneling effective mass also increases, and thus, the curvature of that complex band increases. So, from Fig. 2(b) and (d), it can also be seen that when d decreases to 2.6$\mathring{A}$ (and 2.0$\mathring{A}$) for AA stack (and AB stack) then that complex band crosses with other bands and the tunneling no longer remain as a direct one.

Now, using the Wentzel–Kramers–Brillouin approximation, the direct tunneling probability for the BTBT process can be approximated as [13]

$$T_{\mathrm{BTBT}} = \exp\left\{-\frac{2}{q\xi}\int_0^{E_g} k\left(E\right)dE\right\} \equiv \exp\left\{-\frac{\xi_I}{\xi}\right\} \quad (1)$$

where q is the electronic charge, ξ is the electric field, $E = 0$ is the valence band edge, $E = E_g$ is the conduction band edge, $k(E)$ is the magnitude of the imaginary wave vector, and $\xi_I = \frac{2}{q}(\int_0^{E_g} k(E)dE)$ is basically the "*least action integral*" which is an intrinsic property of the material. As a result, in any applied electric field, controlled by a third terminal (the gate) in the TFET applications, T_{BTBT} can be figured out instantly when it is enumerated.

Now, we investigate the performance of the symmetric DG TFET with an HBL as the channel material [see Fig. 1(a)] with an oxide thickness of t_{ox}. The source region is heavily n^+ doped and drain is heavily p^+ doped, whereas, the channel of length L_{ch} is intrinsic. We also consider that, in an electrostatically well-designed device, the Fermi level is at the conduction band edge (E_c) at the n^+ source and at the valence band edge (E_v) at the p^+ drain, whereas, it is at the midgap of the intrinsic channel at thermal equilibrium. The surface potential profile Ψ_s in this DG TFET is dictated by the Poisson equation [15]

$$\frac{d^2\Psi_s}{dx^2} - \frac{\Psi_s - V_g + V_{bi}}{\lambda^2} = 0 \quad (2)$$

where x is the direction along the channel, V_g and V_{bi} ($\approx \frac{E_g}{2q}$) are the gate and built-in potentials, respectively, and λ is the natural length scale of the potential variation and is given by $\lambda = (\frac{\varepsilon}{2\varepsilon_{ox}}(1 + \frac{\varepsilon_{ox}}{4\varepsilon}\frac{d}{t_{ox}})t_{ox}d)^{\frac{1}{2}}$. Here, ε and ε_{ox} are the channel and oxide dielectric constants, respectively. Applying the boundary conditions: [5] 1) zero electric field at $x = \pm\infty$ and 2) continuous electric field and potential at the source–channel and drain–channel junction, and, the assumption $L_{ch} \gg \lambda$, (2) can be solved analytically and leading to a solution of the form $\Psi_s \propto \exp(-\frac{x}{\lambda})$. The electric field calculated from the surface potential profile can then be given by $\xi = \frac{1}{2\lambda}(\frac{E_g}{2q} - V_g)e^{-\frac{x}{\lambda}}$. From the expression of λ, it can be seen that the use of high-κ gate dielectric and atomically thin planer channel materials will improve the device performance very significantly [16]. It should be noted that the change in Ψ_s at $L_{ch}/2$ should not depend on drain voltage for the proper BTBT process in the TFET operation, which can be achieved by $L_{ch} \gg \lambda$ and by scaling the device in the quantum capacitance limit [8].

Considering HfO_2 as a dielectric ($\varepsilon_{ox} = 25\varepsilon_0$, $t_{ox} = 2$ nm) and an AA-stacked HBL having $d = 2.85\mathring{A}$ as a channel ($L_{ch} = 15$nm), the computed band diagrams for a symmetric n^+-i-p^+ DG TFET are shown in Fig. 3(a) for the OFF-state at $V_g = 0$ and in Fig. 3(b) for the ON-state at $V_g = -0.35$V with a supply voltage V_d of 0.1V. It can be seen from Fig. 3(b) that, under this condition, the reverse bias V_g opens an energy window, $\Delta\Phi$, through which the effective tunneling current flows and this $\Delta\Phi$ can be derived as ($qV_g - \frac{E_g}{2}$). It should also be noted that, this $\Delta\Phi$ is derived here for relatively small V_g so that the effective electric field does not change appreciably from its equilibrium value. Under these circumstances, the BTBT tunneling current can then be written in the form [2], [13]

$$I_{\mathrm{BTBT}} = \frac{g_s g_v q}{h}\int_0^{\Delta\Phi} T_{\mathrm{BTBT}}\left\{f_i\left(E\right) - f_f\left(E\right)\right\}dE \quad (3)$$

in which h is the Planck's constant, $g_s = g_v = 2$ are the spin and valley degeneracies, respectively, and $f_i(E)$ and $f_f(E)$ are the Fermi functions of the initial and final states from and to which the tunneling occurs, respectively. Using (1) and (3), taking $\Delta\Phi$ and ξ across the source–channel junction (x=0) from the band diagram calculations for different d, the drain current I_D at T=300 K can then be calculated as a function of the V_g. It can be seen from Fig. 3(b) that, to open an energy window for tunneling, a reverse bias $V_g = \frac{E_g}{2q}$ is required. So, to compare the ON-current performances for different d, in Fig. 3(c)– (d), we have presented the variation of the direct BTBT current as a function of ($V_g - \frac{E_g}{2q}$) for the AA- and AB-stacked HBL at a

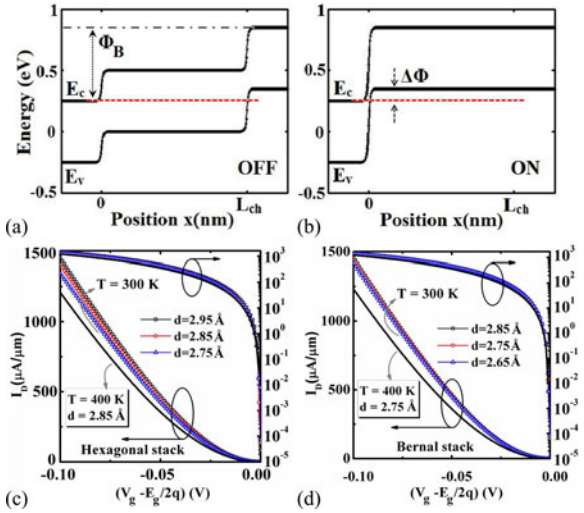

Fig. 3. Energy band diagrams for a symmetric n^+-i-p^+ DG TFET having an AA-stacked HBL of $d = 2.85\mathring{A}$ as a channel material in (a) OFF-state and (b) ON-state, respectively. Transfer characteristics in DG TFET having (c) AA-stacked and (d) AB-stacked HBL as channel materials at $V_d = 0.1$ V and $T = 300K$ for different d. The solid black line shows the ON current at $T = 400K$.

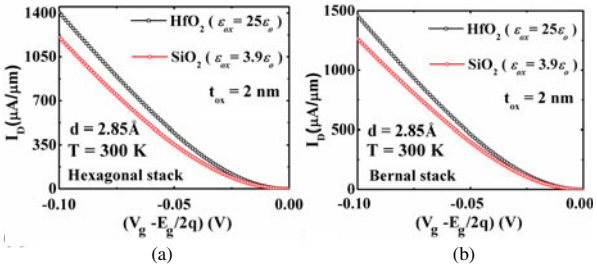

Fig. 4. Comparison of ON current performances in an HBL TFET for two different gate dielectrics, HfO_2 and SiO_2, having same oxide thickness of $t_{ox}=$ 2 nm.

supply voltage $V_d = 0.1$V. It is worth noting that as the d decreases both E_g (ξ_I also) and ε increases, and thus, if we see the variation as a function of V_g only then lowest E_g will provide highest current for a particular V_g. Fig. 3(c)– (d) also reveals that the deviation in the ON-currents due to the increase of band gaps is significantly less. It is found that the ON current deviates nearly 8% for an AA-stacked HBL if we decrease d from 2.95 to $2.75\mathring{A}$ at a value $(V_g - \frac{E_g}{2q}) = -0.1V$, whereas, an AB-stacked HBL shows only 3% deviation, if we decrease d from 2.85 to $2.65\mathring{A}$. Thus, irrespective of the controllability in interlayer distances by the experimental techniques, these GBLs can afford much higher ON current for a range of interlayer distances which makes it easy to use in the efficient TFET applications. It is further observed from Fig. 4 that the ON-current performance increases $\sim 20\%$ due to the change in λ for the use of high-κ HfO_2 instead of low-κ SiO_2 for an oxide thickness, $t_{ox}=$ 2 nm. One can also find that in comparison to the GNR TFET [5], the HBL TFETs provide much higher ON currents. Again, if the OFF-state leakage current is assumed due to the thermionic emission over the barrier Φ_B between the source and drain [see Fig. 3(a)], then the leakage current [5] leads to a value of 56pA/μm for an AA-stacked HBL having $d = 2.85\mathring{A}$ which shows an ON-to-OFF ratio of seven orders of magnitude at room temperature. Furthermore, if the temperature dependence of the dispersion relationship is neglected [17], then, ξ_I and T_{BTBT} remain same for a particular electric field. However, due to the presence of temperature factor in the Fermi function within the current (3) tunneling current decreases with increasing temperature as seen in Fig. 3(c)– (d). As the leakage current of these TFETs is considered due to thermionic emission, with the decrease of temperature the leakage current also decreases quite significantly. An average SS less than 3 mV/dec (extracted from the I_D–V_g characteristics using the same method as in [16]), shows the immense potential of the HBL-based TFETs for realizing high-performance LSTP appliances.

III. Conclusion

Studying the complex bands within the tunable band gap of both the AA- and AB-stacked HBL, we demonstrate that direct BTBT is possible above some critical interlayer spacing. It is explored that the high-ON current and very low-SS value in the HBL TFETs can achieve high-performance LSTP applications.

References

[1] A. M. Ionescu and H. Riel, "Tunnel field-effect transistors as energy-efficient electronic switches," *Nature*, vol. 479, no. 7373, pp. 329–337, 2011.

[2] J. Knoch, S. Mantl, and J. Appenzeller, "Impact of the dimensionality on the performance of tunneling FETs: Bulk versus one-dimensional devices," *Solid State Electron*., vol. 51, no. 4, pp. 572–578, 2007.

[3] A. Schenk "Rigorous theory and simplified model of the band-to-band tunneling in silicon," *Solid State Electron*., vol. 36, pp. 19–34, 1993.

[4] J. Appenzeller, Y. M. Lin, J. Knoch, and P. Avouris, "Band-to-band tunneling in carbon nanotube field-effect transistors," *Phys. Rev. Lett*., vol 93, no. 19, pp. 196805-1–196805-4, Nov. 2004.

[5] Q. Zhang, T. Fang, H. Xing, A. Seabaugh, and D. Jena, "Graphene nanoribbon tunnel transistors," *IEEE Electron Device Lett*., vol. 29, no. 12, pp. 1344–1346, Dec. 2008.

[6] A. C. Seabaugh and Q. Zhang, "Low-voltage tunnel transistors for beyond CMOS logic," *Proc. IEEE*, vol. 98, no. 12, pp. 2095–2110, Dec. 2010.

[7] Y. Zhang, T. T. Tang, C. Girit. Z. Hao, M. C. Martin, A. Zettl, M. F. Crommie, Y. R. Shen, and F. Wang, "Direct observation of a widely tunable bandgap in bilayer graphene," *Nature*, vol. 459, no. 7248, pp. 820–823, 2009.

[8] G. Fiori and G. Iannaccone, "Ultralow-voltage bilayer graphene tunnel FET," *IEEE Electron Device Lett*., vol. 30, no. 10, pp. 1096–1098, Oct. 2009.

[9] Y. Fan, M. Zhao, Z. Wang, X. Zhang, and H. Zhang, "Tunable electronic structures of graphene/boron nitride heterobilayers," *Appl. Phys. Lett*, vol. 98, pp. 083103-1–083103-3, 2011.

[10] C. Bjelkevig, Z. Mi, J. Xiao, P. A. Dowben, L. Wang, W. N. Mei, and J. A. Kelber, "Electronic structure of a graphene/hexagonal-BN heterostructure grown on Ru(0001) by chemical vapor deposition and atomic layer deposition: Extrinsically doped graphene," *J. Phys.: Condens. Matt*., vol. 22, no. 30, pp. 302002-1–302002-6, 2010.

[11] E. Kan, H. Ren, F. Wu, Z. Li, R. Lu, C. Xiao, K. Deng, and J. Yang, "Why the band gap of graphene is tunable on hexagonal boron nitride," *J. Phys. Chem. C*, vol. 116, no. 4, pp. 3142–3146, 2012.

[12] Atomistix ToolKit (ATK), QuantumWise simulator. (2013). [Online]. Available: http://www.quantumwise.com

[13] R. K. Ghosh and S. Mahapatra, "Direct band-to-band tunneling in reverse biased MoS_2 nanoribbon p-n junctions," *IEEE Trans. Electron Devices*, vol. 60, no. 1, pp. 274–279, Jan. 2013.

[14] M. Luisier and G. Klimeck, "Simulation of nanowire tunneling transistors: From the Wentzel-Kramers-Brillouin approximation to full-band phonon-assisted tunneling," *J. Appl. Phys*., vol. 107, pp. 084507-1–084507-6, 2010.

[15] K. Suzuki, T. Tanaka, Y. Tosaka, H. Horie, and Y. Arimoto, "Scaling theory for double-gate SOI MOSFET's," *IEEE Trans. Electron Devices*, vol. 40, no. 12, pp. 2326–2329, Dec. 1993.

[16] N. Patel, A. Ramesha, and S. Mahapatra, "Drive current boosting of n-type tunnel FET with strained SiGe layer at source," *Microelectron. J*., vol. 39, no. 12, pp. 1671–1677, 2008.

[17] R. Capaz, C. D. Spataru, P. Tangney, M. L. Cohen, and S. G. Louie, "Temperature dependence of the band gap of semiconducting carbon nanotubes," *Phys. Rev. Lett*., vol. 94, pp. 036801-1–036801-4, 2005.